Acta Materialia 100 (2015) 73–80

Contents lists available at ScienceDirect

Acta Materialia

journal homepage: www.elsevier.com/locate/actamat

Transition from shear to stress-assisted diffusion of copper–chromium nanolayered thin films at elevated temperatures

R. Raghavan [a,*], J.M. Wheeler [b,c], T.P. Harzer [a], V. Chawla [b], S. Djaziri [a], K. Thomas [b], B. Philippi [a], C. Kirchlechner [a], B.N. Jaya [a], J. Wehrs [b], J. Michler [b], G. Dehm [a]

[a] Max-Planck-Institut für Eisenforschung GmbH, Structure and Nano-/Micromechanics of Materials, Max-Planck-Strasse 1, 40237 Düsseldorf, Germany
[b] Empa, Swiss Federal Laboratories for Materials Science and Technology, Laboratory for Mechanics of Materials and Nanostructures, Feuerwerkerstrasse 39, CH-3602 Thun, Switzerland
[c] Laboratory for Nanometallurgy, Department of Materials Science, ETH Zürich, 8093 Zurich, Switzerland

ARTICLE INFO

Article history:
Received 3 July 2015
Revised 10 August 2015
Accepted 11 August 2015

Keywords:
Micromechanics
Nanostructured materials
Interfaces
Stress-assisted diffusion

ABSTRACT

The mechanical behavior of Cu–Cr nanolayered films and an alloy film of nominal composition $Cu_{20}Cr_{80}$ at.% was studied by microcompression testing at temperatures from 25 °C to 300 °C. Comparing nanolayered films, plastic deformation and failure occurred at consistently higher stress levels in the film with the smaller layer thicknesses. Plasticity in the nanolayered films always initiated in the softer Cu layers followed by a finite strain-hardening response in the stress–strain curves. Failure indicated by a strain-softening response following the higher peak strength due to shearing and tearing at columnar boundaries of Cr was observed in the nanolayered films at 25 °C and 100 °C. A transition from shearing and crack formation across the Cu–Cr interfaces leading to anomalous grain growth or beading of the nanocrystalline Cu layers was observed at elevated temperatures of 200 °C and 300 °C. On the other hand, the $Cu_{20}Cr_{80}$ at.% alloy film exhibited failure by columnar buckling consistently at elevated temperatures, but shearing promoted by buckling at the highest strengths among the films at ambient temperature.

1. Introduction

The mechanical behavior of nanolayered films is gaining increasing interest in the scientific community, because they serve as model systems to clarify the role of interactions between the defect structure, crystallinity and the various boundaries or interfaces on the mechanical properties of the films. Several insights into these interactions in terms of threading and misfit dislocation dynamics with intra-layer grain boundaries, interlayer interfaces, vacancy concentration, etc. [1] have indeed been obtained from detailed investigations into the small-scale mechanical behavior of several metal–metal [2–6] and metal-ceramic [7–10] combinations of nanolayered films. Nevertheless, since the nanostructure of these films is not a state variable and depends on the processing route of the films, the aforementioned insights into the mechanical response of nanolayered films still pose numerous fundamental questions. The change in dislocation dynamics with temperature, which leads to transitions in deformation mechanisms of the nanolayered films [11–16], adds another dimension of complexity. In addition, the study of metallic nanolayered thin films with mutually immiscible systems [17,18] holds promise of improving the thermo-mechanical stability of metallic nanostructured alloys [19].

Pure nanocrystalline Cu layers confined within stiffer layers such as W and TiN exhibit a transition from shear to diffusion dominated flow at low homologous temperatures ($T/T_m < 0.4$) [11,12]. A recent study showed that a similar thermal transition in deformation mechanism is expected, when stiffer Cr layers confine the Cu layers too [17]. But, in contrast to the W and TiN containing nanolayered (NL) films, the stress-driven diffusion at elevated temperatures was observed to be inhomogeneous in the Cu–Cr system. The nanocrystalline Cu layers broke through the weak intercolumnar Cr boundaries, forming Cr segments and connected across within the deformed regions. In other words, uniform lateral flow perpendicular to the loading direction and coarsening into nanocrystals on the outer surface was not observed in the Cu–Cr system. Here we investigate whether this behavior is dependent on the nominal composition or the thickness ratio of the nanolayered film.

* Corresponding author.
E-mail address: r.raghavan@mpie.de (R. Raghavan).

http://dx.doi.org/10.1016/j.actamat.2015.08.016
1359-6454/

2. Materials and methods

2.1. Film synthesis

Two nearly 2 μm thick nanolayered (NL) thin films with thickness ratio of 1:4 and nominal composition of $Cu_{20}Cr_{80}$ at.% (20 nm Cu//80 nm Cr and 10 nm Cu//40 nm Cr denoted as 20Cu//80Cr–NL and 10Cu//40Cr–NL hereafter) were deposited by direct current magnetron sputtering (Mantis Deposition Ltd., UK, Model: QPrep) on Si (100) substrates with a 200 nm thick thermally grown SiO_2 buffer layer (Table 1). An alloy film of the same nominal composition was deposited on similar substrates by simultaneous sputtering of the Cu and Cr targets (denoted as Cu_{20}-Cr_{80}–A hereafter). The films were synthesized by sputtering 99.99% pure copper and 99.95% pure chromium targets (76.2 mm diameter × 3 mm thick) in an Ar atmosphere with a flow rate of 45 sccm and sputtering pressure was 2.9×10^{-3} mbar after achieving a base pressure better than 9×10^{-8} mbar. Currents of 200 mA and 300 mA were used for Cu and Cr respectively for the NL films. In addition, the substrates were rotated at a constant speed to achieve a uniform deposition.

2.2. Structural characterization

High-resolution scanning electron microscopy (HRSEM) images of cross-sections of the films were obtained at a tilt of 54° by using a Zeiss Auriga® cross-beam workstation. The cross-sections were made using the Ga^+ beam operated at 30 kV with currents of 2 nA to mill the rectangular trenches, fine mill the walls with 600 pA and polish using 50 pA. Surfaces of the films were polished using the Ga^+ beam with currents of 50 pA operated at 30 kV before imaging.

Grazing incidence X-ray diffraction (Bruker AXS, D8 Discover) was used to determine the crystal structure of the films by using Cu-K_α (λ = 1.5418 Å) radiation to characterize the films. An excitation voltage of 40 kV and current of 40 mA were used with a constant angle of incidence of 2°. The scans were performed using a step size of 0.02° and scan range from 20° to 90° respectively.

Transmission electron microscopy (TEM) of cross-sections of the thin films was carried out using a Jeol JEM-2200FS field emission gun instrument operated at 200 kV. Details of the procedure for preparing the electron transparent cross-section lamellae and TEM energy dispersive X-ray spectroscopy (EDS) measurements are provided in Ref. [20].

2.3. Microcompression

Micro-pillars were machined within the films using a Zeiss Auriga® dual beam FIB workstation and the compression tests were carried out by using the Alemnis GmbH *in situ* SEM indenter [21,22]. The details of the machining and compression parameters are the same as in Ref. [17]. The load–displacement curves were corrected for instrument and substrate compliances [23] before converting them into engineering stress–strain curves using diameters at ≈60% of the height of the micropillars. Stress values at 0.5% strain offsets of the engineering stress–strain curves were considered as the yield strengths of the respective films. The micropillars were imaged after compression with a Hitachi S-4800 high-resolution scanning electron microscope. To obtain further insights into the deformation mechanisms, the compressed micropillars were sectioned along the length of the micropillars using currents of 50–60 pA and imaged using the Gemini® electron column of the Zeiss dual beam FIB workstation.

Table 1
Summary of microstructural parameters characterized using TEM.

Film	Layer thickness, l (nm)		Grain size, d (nm)	
	Cu	Cr	Cu	Cr
10Cu//40Cr–NL	11 ± 1	38 ± 1	12 ± 2	20 ± 3
20Cu//80Cr–NL	21 ± 2	79 ± 1	21 ± 3	36 ± 6
$Cu_{20}Cr_{80}$–A	–	–	90 ± 27 (column width)	

3. Results and interpretation

3.1. Nanostructure of the films

The XRD patterns of 10Cu//40Cr–NL, 20Cu//80Cr–NL and Cu_{20}-Cr_{80}–A films are shown in Fig. 1. The NL films exhibit three intense Bragg reflections, (110), (200) and (211) which belong to the Cr layers and few Cu peaks (111), (200) and (220) with weak and attenuated intensity at high diffraction angles. The XRD pattern of the $Cr_{80}Cu_{20}$–A film shows only a single reflection, which is attributed to (110) *bcc* Cr with the aid of TEM investigations described next.

Cross-sectional TEM of the NL films confirm the nanocrystalline nature and minimal interfacial porosity (Fig. 2a and b), as compared to the NL films with a nominal composition of $Cu_{66}Cr_{34}$ used in an earlier study [17]. In addition, the arcing of the Cu {111} and overlapping Cr {110} reflections in the diffraction patterns [24] indicate the presence of ⟨111⟩ fiber texture within both the nanolayered films. Also, the orientation relationship between the Cu {111} and Cu {200} reflections indicate the presence of {111} twin variants of Cu [25]. Note that Fig. 2b also revealed that a Cu layer was unintentionally omitted during the synthesis of the 10Cu//40Cr–NL film. The $Cu_{20}Cr_{80}$–A film exhibited a fine grained structure close to the film-substrate interface, which grew in the form of columns with a width of 90 ± 27 nm near the top of the film (Fig. 2c). The corresponding diffraction pattern indicated that the alloyed film possesses a *bcc* crystal structure. Scanning TEM-EDS measurements confirmed the formation of a supersaturated solid solution of the alloy film, and chemically distinct, but wavy interfaces within the NL films. The apparent mixing at the Cu–Cr interfaces in the 10Cu//40Cr–NL film is a measurement artifact due to the combined effects of the interaction volume of signal generation and thermal drift of the sample during EDS acquisition understood as follows. Due to inelastic scattering events, the beam "broadens" on its way through the sample. Thus, X-rays excited from that regions will also contribute to the spectra [26]. Hence, the interface is assumed to be atomically abrupt.

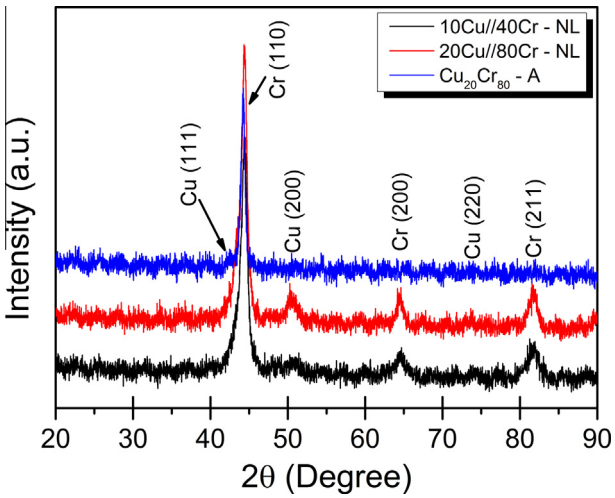

Fig. 1. GI-XRD patterns of the NL and alloyed films.